

## Smartphone based health accessory for colorimetric detection of biomarkers in sweat and saliva†

Cite this: *Lab Chip*, 2013, 13, 3232

Vlad Oncescu,<sup>‡a</sup> Dakota O'Dell<sup>‡b</sup> and David Erickson<sup>\*a</sup>

The mobile health market is rapidly expanding and portable diagnostics tools offer an opportunity to decrease costs and increase the availability of healthcare. Here we present a smartphone based accessory and method for the rapid colorimetric detection of pH in sweat and saliva. Sweat pH can be correlated to sodium concentration and sweat rate in order to indicate to users the proper time to hydrate during physical exercise and avoid the risk of muscle cramps. Salivary pH below a critical threshold is correlated with enamel decalcification, an acidic breakdown of calcium in the teeth. We conduct a number of human trials with the device on a treadmill to demonstrate the ability to monitor changes in sweat pH due to exercise and electrolyte intake and predict optimal hydration. Additionally, we perform trials to measure salivary pH over time to monitor the effects of diet on oral health risks.

Received 6th April 2013,  
Accepted 7th June 2013

DOI: 10.1039/c3lc50431j

[www.rsc.org/loc](http://www.rsc.org/loc)

### Introduction

The cost of healthcare in the U.S. is projected to reach 30% of the GDP by 2040.<sup>1</sup> The widespread adoption of smartphones among nearly all age and income groups presents an opportunity for the development of mobile health applications and accessories for these devices that can help reduce costs and improve the accessibility of healthcare. Over 40 000 mobile health applications (commonly referred to as “apps”) are currently available and that number is expanding rapidly.<sup>2</sup> A number of consumer mobile health accessories that integrate with smartphones such as Nike FuelBand, Fitbit One, and Misfit Shine combine accelerometers, heart rate monitors, and data on oxygen consumption to give users information on physical activity and daily calorie expenditure. Despite the amazing pace of developments in mobile health technologies, however, the vast majority of devices on the market focus exclusively on these physical measurements.

A high-impact area for mobile health, that has not yet taken off commercially, is in the development of biochemical portable diagnostics tools.<sup>3</sup> Smartphone accessories for the detection of biomarkers in bodily fluids could greatly reduce the cost of medical testing and increase global access to healthcare. Several academic groups are currently developing smartphone platforms for biomarker detection. Recently, Coskun *et al.*<sup>4</sup> have developed a testing platform that can be

used at home to test foods for peanut traces and other common allergens. Several other groups are working on smartphone-based image processing for quantifying colorimetric changes on paper-based immunoassays.<sup>5</sup>

In this paper, we demonstrate an integrated smartphone accessory for monitoring changes in sweat and salivary pH. In addition, numerous academic publications have also studied the relationship between pH and various physiological conditions. For example, salivary pH is an important factor on enamel decalcification<sup>6,7</sup> and sweat pH can be used to indicate the risk of dehydration.<sup>8</sup>

The smartphone accessory presented here has an integrated design that allows noninvasive real-time analysis using disposable test strips. In this paper, we first introduce the system and how it integrates with existing smartphones. Second, we describe the software for colorimetric detection and the method through which we ensure uniform repeatable results on different smartphones. Finally, in the results section, we show the applicability of our system to sweat and saliva biomarker detection through a series of human trials. We demonstrate that our system can be used in the context of sweat testing in order to prevent the risk of dehydration and to improve performance during physical activity and in the context of saliva testing can be used to evaluate the impact of diet changes on oral health.

### Methods

#### Overview of the system

The system presented here consists of a smartphone case, application, and test strips. The case has a slot in which a test strip can be inserted for colorimetric analysis using the

<sup>a</sup>Sibley School of Mechanical and Aerospace Engineering, Cornell University, Ithaca, NY 14853, USA. E-mail: [de54@cornell.edu](mailto:de54@cornell.edu)

<sup>b</sup>School of Applied and Engineering Physics, Cornell University, Ithaca, NY, 14853, USA

† Electronic supplementary information (ESI) available. See DOI: 10.1039/c3lc50431j

‡ These authors have contributed equally to this paper.

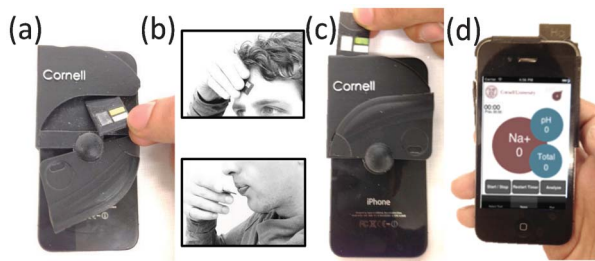


**Fig. 1** (a) Picture of the device with the user removing a test strip from the back storage compartment. (b) Sweat sample acquisition by application of the test strip on the forehead or saliva sample acquisition by user spitting on the test strip. (c) Insertion of the test strip in the optical system for reading. (d) Analysis of the pH once the test strip is inserted using the iPhone app.

cellphone camera and a space to store up to 6 additional test strips. Fig. 1 shows a user removing a test strip from the storage space, collecting a sweat or saliva sample, and inserting the test strip in the device for analysis. The test strips incorporate 3 different elements inserted in a 3D printed support: an indicator strip, a reference strip and a flash diffuser. As an initial application presented here, we have designed the test strips in order to measure pH differences in sweat and saliva. The indicator strip consists of a 9 mm by 4 mm cutout of a pHydrion Spectral 5.0 to 9.0 plastic pH indicator strip for sweat testing and a 1.0 to 14.0 strip for saliva testing. The reference strip is made of white plastic material and is used in order to detect changes in white balance on the iPhone camera due to different light conditions or user error. The flash diffuser consists of a 2 mm thick membrane of polydimethylsiloxane (PDMS). The purpose of the flash diffuser is to reduce variations in the reading for different lighting conditions and will be explained in the calibration section of this paper. It allows light from the smartphone's

flash to diffuse and illuminate the back of the tests strip uniformly. In addition, the case is 3D printed using opaque Vera black material in order to isolate the test strip from variable external light.

### Smartphone application

To work with the accessory, we have developed a software app to handle image acquisition and processing, and data storage and manipulation. The app shown in Fig. 2 works as follows. First, upon loading the app, the user selects the test strip being used from a menu of different biomarker tests available, and the app loads the appropriate calibration data and user interface. Secondly, the user inserts the disposable test strip cartridge into the hardware accessory and touches the “Analyze” function on-screen. Thirdly, the app turns on the camera flash and takes an image of the test strip. The quantitative biomarker concentration is determined from the image (see “Colorimetric quantification” section) and displayed on screen in under five seconds. If pertinent to the specific biomarker, additional post-processing is also done from the biomarker results, and these results are displayed alongside the biomarker concentration. Finally, by swiping left, a scatter plot of the results is generated to show trends over time. If desired, the data set can also be sent *via* email for later viewing or additional analysis.

### Colorimetric quantification

Although the ubiquity of smartphones with high-quality integrated cameras makes such devices ideal for point-of-care biomarker detection, the wide range of variations across different devices and of test strip illumination present significant challenges to accurate colorimetric quantification. Other investigators have addressed this problem by calibrating for ambient light conditions through conversion to color spaces which are less sensitive to changes in brightness.<sup>5,9</sup> On

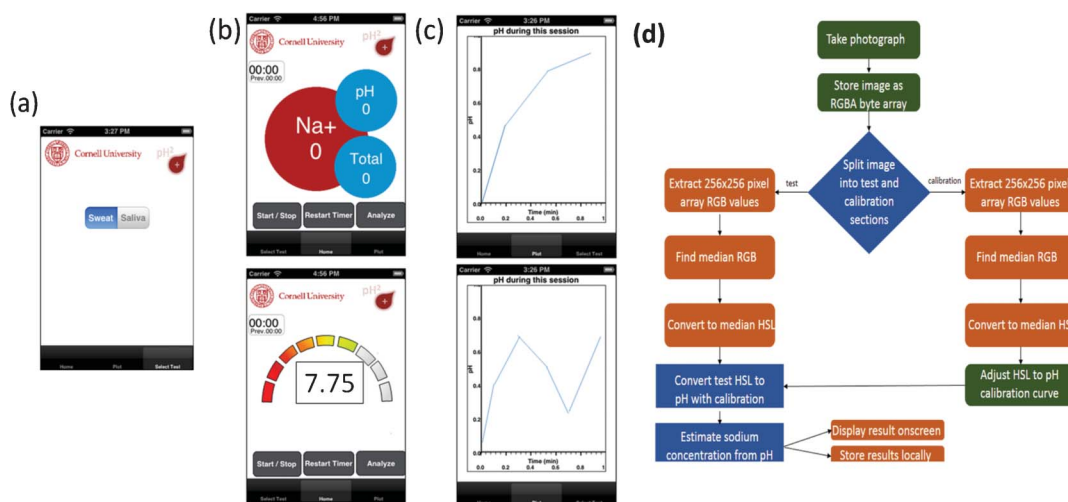


**Fig. 2** An overview of the modular smartphone app and its operation. (a) The user selects the desired test strip from a menu of pre-calibrated test options. (b) The app automates the process of image acquisition and processing for the desired application. The top image shows the sweat pH and electrolyte interface; the bottom, the salivary monitoring interface. (c) A plot of the data is produced to demonstrate trends over time. (d) A schematic overview of the image acquisition and processing algorithm.

its own, this approach still requires uniform external illumination, and false colorimetric readings can be made if the phone is not placed at the proper distance from the test strip.<sup>5</sup> One of the unique opportunities of smartphone-based colorimetric detection for portable diagnostics, however, is that image acquisition can instead be automated, so that the test strip is always held in the ideal position and imaged in the same manner, and the data is not easily affected by deviations in user protocol. Our device is isolated from ambient light with the hardware accessory and diffuses light from the smartphone camera flash for reproducible and uniform illumination, improving measurement accuracy and minimizing the potential for user error (see “Calibration” for details).

While the use of the camera flash instead of external light removes much of the variability from the image acquisition, there are additional steps which must be taken for accurate quantitative processing. Although the image from the smartphone camera is initially defined with RGB (red green blue) values, individual red, green, and blue channels do not correlate well with pH over the range of a universal indicator strip. Nevertheless, the RGB values can be readily converted to an alternate color space that matches the color spectrum of the test strips more closely. We chose to convert to hue, which unlike RGB was found to monotonically increase with pH in our experiments over the entire range of the colorimetric test strips used, as can be seen in Fig. S1 of the ESI.† This advantage of the hue value over RGB for smartphone-based colorimetric imaging has also been recently demonstrated by Chang.<sup>10</sup> In addition, recent work by Cantrell *et al.*<sup>11</sup> has also found hue to be more precise than RGB values for quantitative analysis and less sensitive to variations in illumination, making it an ideal candidate for our colorimetric test strip analysis. After an initial calibration to determine the relationship between the hue and the analyte concentration for each test strip, this single hue value is sufficient to quantitatively specify the color with a high degree of accuracy.

The process of image analysis is as follows. When the “Analyze” button is pressed, the smartphone app activates the camera flash, and an image is captured and stored first as an RGBA (red green blue alpha) byte array. The alpha channel, which is a measure of transparency, is discarded as it does not vary with analyte concentration. The RGB array is split into two sections—the first, corresponding to the upper colorimetric test strip, and the second, to a lower reference region of known color value which is used to compensate for variations between different smartphone cameras and from automated camera adjustment functions such as white balance. A  $256 \times 256$  pixel square is selected from the center of each of these sections, and the hue value is calculated for each pixel from the RGB channels. The hue values are sorted, and the median value is chosen to minimize any remaining edge effects which are not removed by the PDMS flash diffuser. Because the color of the plastic reference section should not change between experiments if the device works correctly, the image acquisition process is restarted if the reference hue value varies from the expected calibration value by more than 5. This serves to eliminate the possibility of a user protocol error—if the test strip is inserted incorrectly and the strip is not optically isolated, the reference check will fail and the data will not be stored. If the reference check is passed, the

test hue value is converted into an analyte concentration by means of a measured calibration curve and the relevant biological information is displayed on-screen immediately. A schematic of this process is given in Fig. 2d.

### Calibration

The correlation between hue and pH is built into the application, allowing users to run tests without additional calibration. This is possible because the case is designed in a way that minimizes the effect of external lighting as was previously discussed. Fig. 3a illustrates the design of the case around the camera and flash that allows for uniform lighting of the test strip. The advantage of using this case design is illustrated by the pictures of the strips in Fig. S2 of the ESI.† By guiding the flash light through the PDMS diffuser on the strip and behind the test strip, we avoid the need to build in a lighting element, such as an LED, that would make the system bulkier and require power input. The strip is imaged at a distance of 2.20 mm from the smartphone's camera and the whole optical piece has a depth of 4.90 mm. The relationship between hue and pH for our test strips was established using buffer solutions and a pH electrode (VWR SympHony SB70P) for an 8 point calibration. Fig. 3b shows the variations in hue readings for 3 different iPhones (models 4 and 4S). The same test strip and holder were used at a given pH for all three iPhones meaning that the differences can be attributed directly to differences in the hardware of the iPhones. A third order polynomial was fitted through the data points in order to obtain a correlation between pH and hue. Fig. 3c shows the maximum deviation of the measured pH from the calibrated values. It was found that the variation between phones is the largest source of error, therefore defining the accuracy of the system over the range of physiologically relevant pH values to be within 0.2 pH units.

As explained previously, in order to further improve the accuracy of our system, we incorporate a white reference strip on our test strip. A large variation in the hue value of the white reference indicates a failed measurement, possibly from a faulty or incorrectly inserted test strip. If the application detects an abnormal hue value, it rejects the data point and signals to the user to take another reading.

Although the system shown here was designed for and prototyped on the iPhone 4 and 4S, it could easily be ported to any other smartphone platform with a CMOS camera. Even if there are systematic differences in camera function and sensitivity between smartphones from different manufacturers, these differences can be corrected by calibrating the hue-to-pH conversion function once for each smartphone model used. If the hardware accessory is re-designed to fit over the camera and properly re-calibrated, the most important metric for determining the accuracy of the device should still be the variation between several phones of the same model, as described above.

## Results and discussion

### Sweat monitoring for hydration and electrolyte loss

It is generally well-accepted that dehydration can negatively impact performance during exercise,<sup>12</sup> however over-hydrating

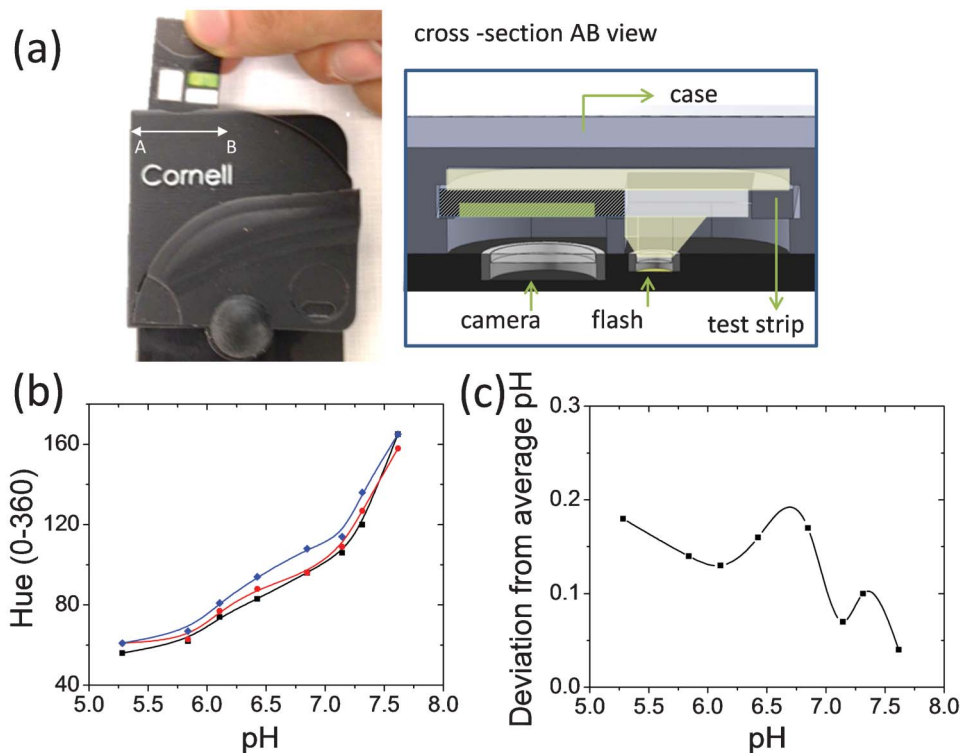


**Fig. 3** (a) Test strip imaging with the first image showing the insertion of the test strip and the second one showing a cross sectional view of the optical system. (b) Hue–pH correlation for 3 different phones. (c) Maximum deviations for three different iPhones from the measured calibration curve.

is similarly dangerous since it can lead to hyponatremia, a disorder resulting from abnormally low sodium plasma concentrations.<sup>13,14</sup> Hyponatremia has resulted in deaths both in athletic competitions and on the battlefield,<sup>15</sup> due to a disruption in the osmotic balance across the blood-brain barrier, resulting in a rapid influx of water into the brain. In addition, studies have shown the sodium concentration of sweat can be used to evaluate the risk of muscle cramps in athletes.<sup>16,17</sup> There is currently no system for accurately monitoring hydration levels or sweat sodium concentrations during exercise. However, there have been several studies showing the correlations between sweat pH and sodium concentration, as well as pH and sweat rate.<sup>18–20</sup> Therefore, by accurately measuring changes in sweat pH during physical exercise, we can determine an optimal hydration strategy.

In a recent paper, Curto *et al.*<sup>21</sup> demonstrated continuous, smartphone-based sweat pH monitoring using a wearable microfluidic platform. A wearable colorimetric pH sensor that can be incorporated directly into clothing has some obvious benefits; there are, however, applications in which a discrete sensing system with disposable cartridges, such as the one presented here, could be more appropriate. The unique use of the diffused smartphone flash in our system allows for easy and consistent imaging, even in the absence of external light. Moreover, the image processing algorithm was designed to require minimum computational power and is performed in real-time directly on the smartphone, without the need to transfer and process the data on an additional computer. While a robust wearable sensor is likely more cost-effective

than disposable strips for a single application, the same accessory presented here could also be used to measure various additional biomarkers in sweat, saliva, or urine, which could ultimately be more cost-effective for an end user than needing separate microfluidic devices for each desired application.

In order to test the system and observe pH changes during exercise we have performed several experiments with users running on a treadmill between 30 and 60 min. The goal was to show that pH variations during exercise are significant and can indicate something about the intensity of the exercise. The participants in this study were all males between the ages of 25 and 37 who run regularly and participate in competitive racing events. Fig. 4a shows pH variations at 3 different run intensities for one user. It shows that at high exercise intensities, characterized by an increased sweat rate, the pH reaches less acidic levels. Fig. 4b shows the variations in pH between 3 users running at the same speed of 6 mph for 30 min. The results indicate that different users exercising in similar ways would need to exert different levels of effort. Fig. 4c shows the effect of cooling down by drinking 20 fl. oz. Gatorade at 40 min during 60 min runs. This is expected since sweating is the body's method to regulate its temperature.<sup>22</sup> Drinking cold fluids decreases the sweat rate and affects the sweat pH.

Because sweat pH has previously been correlated to the concentration of sodium,<sup>18</sup> the experimental measurements of pH presented here also give the approximate sodium concentration of the sweat at each stage throughout the run.



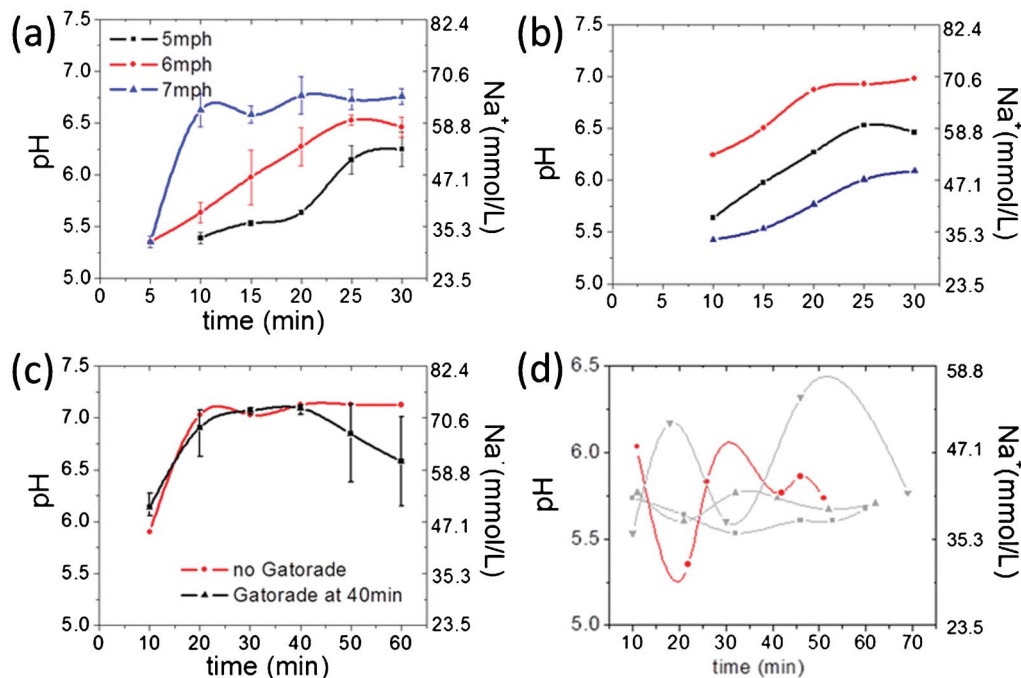


**Fig. 4** (a) pH and sodium concentration variations for runs at different intensities. (b) Variations between 3 different users running at 6 mph. (c) Effect of cooling down with intake of 20 fl oz of Gatorade 40 min into the run for one user. Sodium levels are derived from ref. 16. (d) Hot yoga trials showing pH variations for 4 users during regular exercise. Red line show variation for a user who started hydrating at 10 min and maintained constant exercise and regular hydration for the remainder of the trial.

The sodium concentration is shown on the right y axis in all the experiments in Fig. 4. It has also been found that the concentrations of the constituent electrolytes in sweat vary proportionally with sweat rate.<sup>19,20</sup> By combining these results, an estimate of both the sodium and water losses over time due to sweating can be obtained. Since different users respond to exercise in different ways, there can be no universal guidelines for hydration and electrolyte intake. Using this system to monitor pH and sodium concentration allows for a better estimation of the fluid and electrolyte intake needed to fully replenish losses.

Additional experiments were performed to monitor the variations in sweat pH in other athletes, such as hot yoga practitioners. Hot yoga is the practice of yoga in hot and humid conditions which allows for easy sample collection and analysis. The users involved in these test trials were all women between 21 and 49 who perform hot yoga more than once a week. The users were instructed to perform exercises at their own pace and hydrate at their will. In Fig. 4d we show variation in sweat pH for the 4 users. The user highlighted in red only started hydrating at the 10 min mark and maintained a constant exercise pace after, hydrating regularly before cooling off during the last 5 min of the trial. The test trials which lasted up to 70 min show the expected patterns of pH variations due to hydration and cooling down periods. The maximum variations were under 1 pH unit and the changes in pH are extremely sensitive to changes in user intensity and hydration. These test trials demonstrate the advantage and applicability of discrete sweat pH measurements in non-

continuous forms of athletic activity. These sudden changes in pH can be easily monitored using the system presented here and analyzed directly on a smartphone.

#### Saliva pH monitoring for preventing enamel decalcification

Another important application for pH monitoring is in preventing enamel decalcification. There have been numerous studies describing the effects of pH on oral health, more specifically on the dissolution of calcium hydroxyapatite, the main inorganic component of dental hard tissues.<sup>23</sup> It is believed that enamel decalcification occurs below a certain critical pH that has previously been experimentally determined to be around 6.2.<sup>24</sup> More recent papers describe the critical pH as a function of calcium concentration in saliva.<sup>25</sup>

Here we demonstrate the potential of our system to monitor changes in salivary pH through the day. Data from one user during a typical day, from early morning (at  $t = 0$  h) until night (at  $t = 16$  h), is presented in Fig. 5a. Periods of food intake resulted in a rapid increase in pH and are highlighted in blue on the plot. Ultimately, the objective of salivary pH monitoring is to enable people to estimate their risk of enamel decalcification and to make suitable changes in their diet. For this purpose, estimating the amount of time the salivary pH is above a certain value is important. Fig. 5b gives this data for 3 different users (all males between the ages of 25 and 37) during a typical day. Fig. 5c shows the impact of diet on saliva pH for one user. Dental research has shown that bacterial interaction with carbohydrates in the mouth results in the formation of acids.<sup>26</sup> The variations between users are a result of differences in diet and exercise, as well as innate metabolic

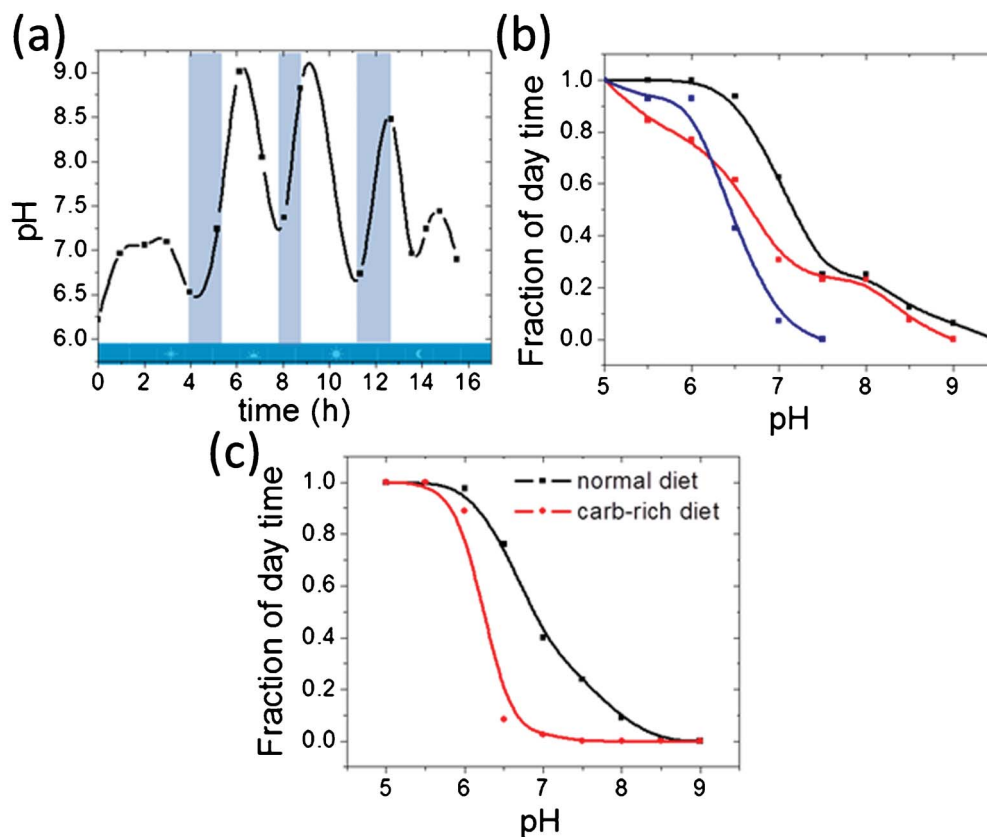


**Fig. 5** (a) Variations in saliva pH over the course of a day for one user. The colored bars indicate periods of food intake. (b) Fraction of the day above a certain pH (data for 3 users). (c) Variation in pH for one user on two different diets (high-carb diet in red, normal diet in black).

differences. Changes in diet for each user, however, have a marked impact on the salivary pH over the course of the day. By monitoring the salivary pH of one user on an ordinary and carbohydrate-rich diet (Fig. 5c), we can see the effect of carbohydrate-induced acid formation on average salivary pH. The device thus offers the potential for personalized tracking of the effects of various lifestyle changes over time.

On a typical balanced diet, the user is above the critical threshold of 6.2 pH for nearly 100% of the day, but this drops down to only half the day on a carb-rich diet, resulting in a substantially greater risk of enamel decalcification. These results indicate that the effect of changes in diet can be accurately measured with our device, thus allowing users to make the necessary dietary adjustments in order to improve oral health.

## Conclusion

In this paper, we have presented a smartphone accessory and app for monitoring pH in sweat and saliva. Sweat pH monitoring is important for proper hydration during physical exercise, while saliva pH monitoring can help users make changes in their diet to prevent enamel decalcification. We have shown through a series of human trials that our system can be used in the context of sweat testing in order to prevent

the risk of dehydration and to improve performance during physical activity. In the context of saliva testing, it can be used to evaluate the impact of dietary changes on the risks of enamel decalcification and overall oral health. Because the device presented allows for reproducible colorimetric detection with minimal user error, we believe that such a system could also be extended to a wide range of biomarkers for other portable diagnostics applications.

## Acknowledgements

The authors would like to acknowledge the support of Michael Kalontarov for the 3D printing of smartphone case. D.E. acknowledges the support of CAREER award #0846489 from the US National Science Foundation. In addition, V.O. acknowledges the support of the National Science and Engineering Research Council of Canada (NSERC) through a Postgraduate scholarship.

## References

- 1 R. W. Fogel, *Journal of Policy Modeling*, 2009, **31**, 482–488.
- 2 S. Fox, *Mobile health 2010*, Pew Internet & American Life Project, 2010.

- 3 A. W. Martinez, S. T. Phillips, G. M. Whitesides and E. Carrilho, *Anal. Chem.*, 2009, **82**, 3–10.
- 4 A. F. Coskun, J. Wong, D. Khodadadi, R. Nagi, A. Tey and A. Ozcan, *Lab Chip*, 2013, **13**, 636–640.
- 5 L. Shen, J. A. Hagen and I. Papautsky, *Lab Chip*, 2012, **12**, 4240–4243.
- 6 N. West, J. Hughes and M. Addy, *Journal of Oral Rehabilitation*, 2008, **28**, 860–864.
- 7 C. Dawes, *Journal-Canadian Dental Association*, 2003, **69**, 722–725.
- 8 R. Morgan, M. Patterson and M. Nimmo, *Acta Physiol. Scand.*, 2004, **182**, 37–43.
- 9 A. García, M. M. Erenas, E. D. Marinetto, C. A. Abad, I. de Orbe-Paya, A. J. Palma and L. F. Capitán-Vallvey, *Sens. Actuators, B*, 2011, **156**, 350–359.
- 10 B.-Y. Chang, *Bull. Korean Chem. Soc.*, 2012, **33**, 549–552.
- 11 K. Cantrell, M. M. Erenas, I. de Orbe-Payá and L. F. Capitán-Vallvey, *Anal. Chem.*, 2009, **82**, 531–542.
- 12 B. Murray, *Journal of the American College of Nutrition*, 2007, **26**, 542S–548S.
- 13 B. Murray, J. Stofan and E. R. Eichner, *Sports Science*, 2003, **88**, 88.
- 14 M. H. Rosner and J. Kirven, *Clin. J. Am. Soc. Nephrol.*, 2007, **2**, 151–161.
- 15 T. P. Garigan and D. E. Ristedt, *Military medicine*, 1999, **164**, 234–238.
- 16 E. R. Eichner, *Sports Medicine*, 2007, **37**, 4–5.
- 17 J. R. Stofan, J. J. Zachwieja, C. A. Horswill, R. Murray, S. A. Anderson and E. R. Eichner, *International journal of sport nutrition and exercise metabolism*, 2005, **15**, 641–652.
- 18 M. J. Patterson, S. D. Galloway and M. A. Nimmo, *Exp. Physiol.*, 2000, **85**, 869–875.
- 19 M. J. Buono, K. D. Ball and F. W. Kolkhorst, *J. Appl. Physiol.*, 2007, **103**, 990–994.
- 20 H. M. Emrich, E. Stoll, B. Friolet, J. P. Colombo, R. Richterich and E. Rossi, *Pediatr. Res.*, 1968, **2**, 464–478.
- 21 V. F. Curto, C. Fay, S. Coyle, R. Byrne, C. O'Toole, C. Barry, S. Hughes, N. Moyna, D. Diamond and F. Benito-Lopez, *Sens. Actuators, B*, 2012, **171–172**, 1327–1334.
- 22 C. Wyss, G. Brengelmann, J. Johnson, L. Rowell and M. Niederberger, *J. Appl. Physiol.*, 1974, **36**, 726–733.
- 23 J. T. Gore, *J. Dent. Res.*, 1938, **17**, 411–421.
- 24 L. Fosdick and A. Starke, *J. Dent. Res.*, 1939, **18**, 417–430.
- 25 P. Anderson, M. Hector and M. Rampersad, *International Journal of Paediatric Dentistry*, 2008, **11**, 266–273.
- 26 B. G. Bibby and T. G. Ludwig, *J. Dent. Res.*, 1957, **36**, 56–60.